AMS-02 Results Support the Secondary Origin of Cosmic Ray Positrons

Kfir Blum,[1,*] Boaz Katz,[1,†] and Eli Waxman[2,‡]

[1]Institute for Advanced Study, Princeton, New Jersey 08540, USA

[2]Department of Particle Physics and Astrophysics, Weizmann Institute of Science, Rehovot 76100, Israel

(Received 7 May 2013; revised manuscript received 13 October 2013; published 20 November 2013)

We show that the recent AMS-02 positron fraction measurement is consistent with a secondary origin for positrons and does not require additional primary sources such as pulsars or dark matter. The measured positron fraction at high energy saturates the previously predicted upper bound for secondary production, obtained by neglecting radiative losses. This coincidence, which will be further tested by upcoming AMS-02 data at higher energy, is a compelling indication for a secondary source. Within the secondary model, the AMS-02 data imply a cosmic ray propagation time in the Galaxy of $<10^6$ yr and an average traversed interstellar matter density of $\sim 1\ \mathrm{cm}^{-3}$, comparable to the density of the Milky Way gaseous disk, at a rigidity of 300 GV.

DOI: 10.1103/PhysRevLett.111.211101 PACS numbers: 98.70.Sa, 95.35.+d, 96.50.sb

Introduction.—The AMS-02 experiment announced a new measurement of the positron fraction (ratio of e^+ to total $e^\pm$ flux) in Galactic cosmic rays (CRs) [1]. The new measurement extends to high energy $E \sim 350$ GeV, with precision significantly superseding earlier experiments [2–4]. The positron fraction is found to increase with energy, apparently saturating at $e^+/e^\pm \sim 0.15$ at $E \sim 200$ GeV.

A rising positron fraction stands in conflict with expectations based on popular diffusion models, assuming a homogeneous diffusion coefficient and a cosmic ray halo scale height that is independent of cosmic ray rigidity (see, e.g., Refs. [5–7]). This conflict has triggered numerous analyses invoking hypothetical primary sources for the positrons such as pulsars and annihilation or decay of dark matter particles.

In this Letter, we point out that the AMS-02 measurement [1] is in fact consistent with the simplest possible estimate due to the one guaranteed e^+ source: the secondary production of e^+ by the collision of high energy primary CRs with ambient interstellar matter (ISM). The main result of this Letter is contained in Figs. 1 and 2. There, AMS-02 $e^+/e^\pm$ and e^+ data at high energy are seen to comply with an upper bound for secondary production, previously derived in Ref. [8] by ignoring the radiative losses of the positrons.

In the rest of this Letter, we outline the derivation of Figs. 1 and 2, explaining why the AMS-02 result provides a strong hint for a secondary positron source. We comment on the implications of a rising positron fraction that is not in conflict with a secondary source. Assuming secondary production, we then highlight the constraints imposed by the new measurement on models of CR propagation in the Galaxy.

AMS-02 and the secondary positron flux.—While the propagation of CRs in the Galaxy is poorly understood, the expected fluxes of secondaries, such as positrons, are tightly constrained by the measurement of other secondaries, such as boron. This results from the fact that (i) different relativistic particles with the same rigidity propagate in a magnetic field in the same way, regardless of the magnetic field configuration, and (ii) the production rates of all secondaries are correlated in a calculable manner.

The measured number densities n_i of stable secondary CR nuclei are proportional to their net local production rate and are thus well described by

$$n_i = \frac{X_{\rm esc} \sum_{j>i} n_j (\sigma_{j\to i}/m_p)}{1 + (\sigma_i/m_p) X_{\rm esc}}, \tag{1}$$

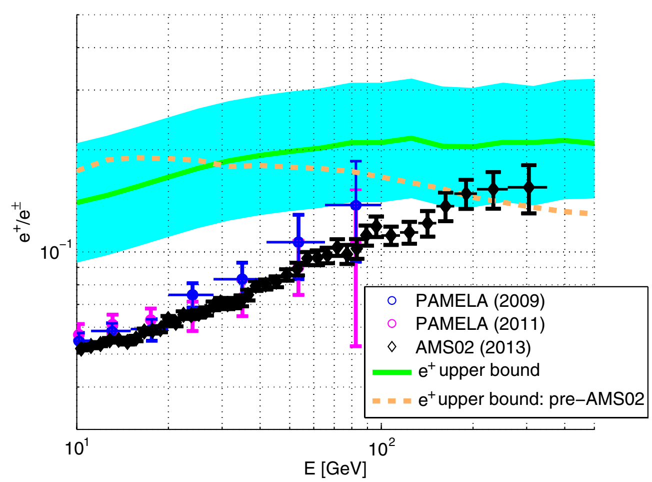

FIG. 1 (color online). Positron flux upper bound vs data, presented in terms of the positron fraction. The theoretical e^+ upper bound, divided by the $e^\pm$ flux measured by AMS-02 [13], is given by the green line. The cyan band shows the estimated calculation uncertainty. The calculation here is identical to that of Ref. [8] but uses the most recent B/C and $e^\pm$ data from AMS-02 [13]. The result of the same calculation using pre-AMS-02 data (B/C ratio of HEAO3 [9] and total $e^\pm$ flux of FERMI [33]) is given by the dashed brown line.

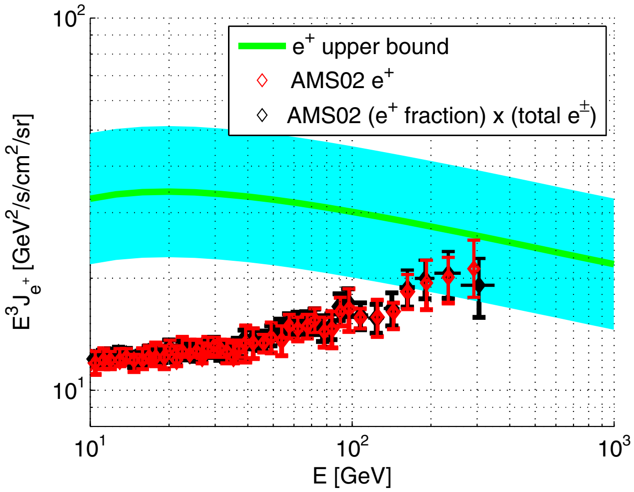

FIG. 2 (color online). The green line with cyan uncertainty band is the same as in Fig. 1, but showing the e^+ flux, rather than the $e^+/e^\pm$ fraction. Red data show the direct AMS-02 e^+ flux measurement [13]. Black data show the e^+ flux obtained by multiplying the $e^+/e^\pm$ fraction by the total $e^\pm$ flux, both taken again from AMS-02.

where $\sigma_{j\to i}$ is the decayed spallation cross section of the parent nucleus j into the secondary i per ISM nucleon, σ_i is the cross section for destruction of i per ISM nucleon, and m_p is the nucleon mass. The grammage $X_{\rm esc}$, defined by Eq. (1), parametrizes the column density of target material traversed by the CRs and is the same for all species. Earlier analyses [9–12] relying on HEAO3 data [9] determined the value of $X_{\rm esc}$ to be

$$X_{\rm esc} = 8.7\left(\frac{E/Z}{10\ \rm GeV}\right)^{-\alpha}\ \rm g\,cm^{-2}, \tag{2}$$

with $\alpha = 0.5$ and different fits varying by $\sim 30\%$ in the range 10 GeV $< E/Z \lesssim$ 100 GeV [9–12]. Here, we use new AMS-02 B/C data [13] to extract the value of $X_{\rm esc}$ up to $E/Z = 1$ TeV. We find (see Ref. [14]) $X_{\rm esc}$ to be given by Eq. (2) with $\alpha = 0.4$, slightly harder in slope than the value deduced from the earlier data.

Equation (1) does not capture the effect of energy loss during propagation. This means that it cannot be directly applied to positrons that are subject to synchrotron and inverse-Compton losses. Nevertheless, it was realized in Ref. [8] that Eq. (1) provides a robust upper limit to the positron flux, given that radiative losses can only decrease the flux of the steep positron spectrum. This upper limit is model independent, derived from data, and requires no free parameters.

The positron fraction measurements of AMS-02 [1] and PAMELA [2,3] are compared to the upper bound of Eq. (1), divided by the total $e^\pm$ flux measured by AMS-02 [13], in Fig. 1. As mentioned above, AMS-02 not only extended the $e^+/e^\pm$ data to higher energy, but it also reported the B/C ratio as well as proton, helium, and individual e^+ and e^- spectra up to hundreds of GeV to TeV. This enables an improved, compared to what was previously possible, calculation of the e^+ upper bound; see Fig. 1. The reported e^+ flux [13] allows us to compare in Fig. 2 the upper bound directly with the data, without involving the e^- flux, which is likely mostly primary and for which there is no definite prediction.

As shown in Figs. 1 and 2 the upper limit is not violated by the new AMS-02 data. This means that the data are consistent with secondary e^+. Moreover, at high energy, the measured e^+ flux saturates within the secondary limit, previously predicted in Ref. [8]. This coincidence, while yet to be further tested by future AMS-02 data at higher energy, is a compelling hint for a secondary source.

It is worthwhile to compare this result to models invoking new primary sources such as pulsars or dark matter. In such models, *ad hoc* tuning of free parameters is required to account for the positron fraction saturating at ~ 0.15 for $E \gtrsim 200$ GeV. The distinction between the secondary and primary models is even more transparent when considering the absolute e^+ flux. In contrast to the $e^+/e^\pm$ fraction that has a limited dynamical range, the e^+ flux due to primary sources could well have been orders of magnitude below or above the secondary bound. We know of no intrinsic scale, and thus of no reason, in any of the primary injection models suggested in the literature, for the e^+ flux to lie close to the data-driven secondary bound, throughout the range $E \sim$ 10–300 GeV.

A $\bar{p}$ consistency check, future tests of the secondary model, and calculation uncertainties.—A test of the validity of our calculations is presented in Fig. 3, where the measured flux of secondary antiprotons [15] that are produced in the same interactions as secondary positrons is compared to the flux obtained from Eq. (1). As seen in the figure, our calculation is consistent with the observations.

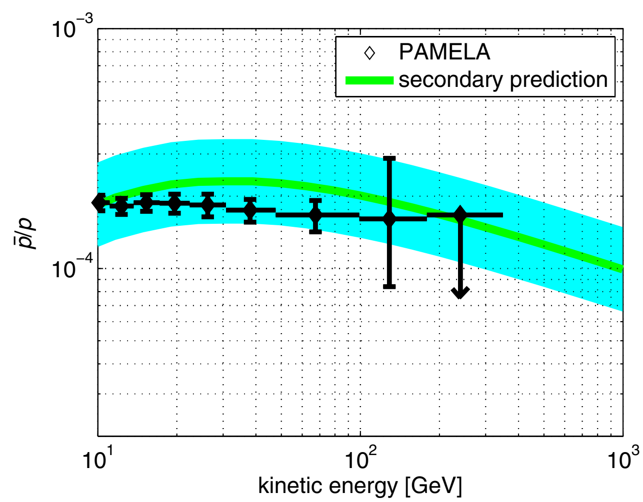

FIG. 3 (color online). PAMELA $\bar{p}/p$ data [15] vs the secondary source prediction of Eq. (1). The cyan band shows an estimated calculation uncertainty on the secondary prediction.

The secondary source hypothesis will be further tested with upcoming AMS-02 measurements of the e^+ and $\bar{p}$ flux at higher energy, up to the TeV range [16]. A potentially useful independent check, although complicated by systematic uncertainties, can be done by analyzing the elemental ratios of nuclei having a radioactive isotope component with a rest frame lifetime of the order of 1 Myr, including Be/B, Cl/Ar, and Al/Mg at high rigidity similar to the cooling time of the positrons [8,17,18]. A more straightforward check, limited, however, to $E/Z \lesssim 10$ GeV, will come from directly measuring the isotopic ratio ^{10}Be/^{9}Be. We note in this context that the early low energy radioactive isotope measurements discussed, for example, in Ref. [19], are limited to $E/Z \lesssim 1$ GeV and so cannot be applied model independently to our study.

We now comment on the systematic uncertainties involved in computing the e^+ upper bound and the $\bar{p}$ flux. We estimate these systematic uncertainties roughly by 50% for both the e^+ and $\bar{p}$ calculations and denote them by the cyan bands in Figs. 1–3. The main potential sources of error are the following.

(i) Different cross section parametrizations for hadron production in pp and pA collisions differ by energy-dependent factors in the order of tens of percent. The difficulty is the inapplicability of perturbative calculations, together with the scarcity of accelerator data for soft charged hadron production at high rapidity. Resolving this ambiguity is beyond the scope of the current Letter. Here, we follow the same calculation done in Ref. [8], to which we refer the reader for more details.

(ii) We expect Eq. (1) to only apply to ~10% accuracy, which is roughly the level at which the assumption of negligible energy change during propagation can be expected to hold for stable secondary nuclei. We also estimate about 30% uncertainty for $X_{\rm esc}$ at 100–500 GeV/nuc. Future AMS-02 data are expected to significantly improve the determination of $X_{\rm esc}$ [16]. While our current parametrization of $X_{\rm esc}$ is consistent with other results [20], the case is not settled, with hints of spectral hardening reported in Refs. [21,22].

(iii) The primary CR nuclei flux and composition at the 0.1–10 TeV/nuc range, responsible for ~10–100 GeV e^+ and $\bar{p}$ production, are still somewhat uncertain [23]. Existing measurements at the relevant range [24–26] differ systematically by 20%–30%. In our analysis, we adopt a proton flux interpolating the preliminary AMS-02 data [13]. These data supersede the earlier PAMELA [24] and CREAM data [26], but as for the B/C, we expect significant updates in the near future.

On a positron fraction rising with energy.—Because of synchrotron and inverse-Compton energy losses, the positron flux is suppressed, compared to the upper bound, by an energy dependent factor $f_{e^+} < 1$. f_{e^+} should increase monotonically as a function of $t_c/t_{\rm esc}$, where t_c is the e^+ radiative cooling time and $t_{\rm esc}$ is the mean propagation time. In the limit $t_c/t_{\rm esc} \gg 1$, we expect $f_{e^+} \to 1$.

The claims in the literature, that the increase with energy of the positron fraction is inconsistent with a secondary origin, are based on two lines of reasoning, neither of which is supported by data (see Ref. [8] for a detailed discussion). The first line of reasoning assumes that (i) primary p and e^- have the same production spectrum, and (ii) primary e^- and secondary e^+ suffer the same energy losses. Both (i) and (ii) are unsubstantiated. It is plausible that primary e^- suffer additional energy loss at the primary CR sources and that the injected e^- spectrum is different than that of the protons. The second line of reasoning adopts some specific propagation model, which leads to $t_c/t_{\rm esc}$ (and so to f_{e^+}) that decreases with energy. Such behavior of $t_c/t_{\rm esc}$ and f_{e^+} can be modified in alternative models.

This discussion makes it clear that given the current AMS-02 data, depicted in Figs. 1 and 2 the call for primary sources is unconvincing. Since both t_c and $t_{\rm esc}$ are neither directly measured nor reliably calculable, the energy dependence of f_{e^+}, and hence of the positron flux, cannot be reliably predicted. The positron data should be regarded as a first direct measurement of f_{e^+}, with interesting implications for the time scales $t_{\rm esc}$ and t_c (see, e.g., Refs. [27,28], and more recently, Refs. [8,18]).

Interpretation: Constraints on CR propagation.—In the rest of this Letter, we assume that the positron flux is of secondary origin and proceed to deduce new constraints on CR propagation.

The secondary model allows us to quantify the amount by which the positron flux is suppressed by propagation energy loss, based on the observations. The suppression factor f_{e^+} is given by the ratio between the observed e^+ flux and the calculated upper bound. This corresponds, in Figs. 1 and 2, to the ratio of the black data to the green curve. We now analyze the constraints arising from Figs. 1 and 2.

(1) CR propagation time: If we ignore Klein-Nishina corrections (see discussion below), then Figs. 1 and 2 imply that

$$t_{\rm esc}(E/Z = 300\ {\rm GeV}) \leq t_c(E = 300\ {\rm GeV}) \sim 1\ {\rm Myr}\left(\frac{\bar{U}_T}{1\ {\rm eV\,cm^{-3}}}\right)^{-1}, \quad (3)$$

$$t_{\rm esc}(E/Z = 10\ {\rm GeV}) > t_c(E = 10\ {\rm GeV}) \sim 30\ {\rm Myr}\left(\frac{\bar{U}_T}{1\ {\rm eV\,cm^{-3}}}\right)^{-1}. \quad (4)$$

The right-hand sides of Eqs. (3) and (4) are based on a rough estimate of the $e^{\pm}$ cooling time at the relevant energies and as such are subject to $O(1)$ uncertainty. Here, $\bar{U}_T$ is the time-averaged total electromagnetic energy density in the propagation region. Note that it is natural to expect that $\bar{U}_T$ should depend on CR rigidity. Thus, $\bar{U}_T$ should be understood as a function of E, although we omit the explicit dependence for clarity of notation.

One irreducible source for energy dependence in the effective value of $\bar{U}_T$ comes from Klein-Nishina corrections that are neglected in Eqs. (3) and (4). The Thomson limit is not a good approximation for 20–300 GeV positrons if $\bar{U}_T$ contains a significant UV component [29]. In that case, the effective radiation energy density for an $\sim$300 GeV e^+ can be significantly lower than that for an $\sim$10 GeV one (see, e.g., Refs. [7,30,31]).

In the top panel of Fig. 4, we plot the cooling time t_c for electrons and positrons under different assumptions for $\bar{U}_T$. Smooth lines set the UV component to zero. Dashed lines show varying amounts of UV light having a blackbody spectrum with a temperature $T = 6000$ K. The bottom panel shows the spectral index of t_c. We learn that significant deviations from the Thomson limit ($d\log t_c/d\log E = -1$) are plausible. In the terms of Eqs. (3) and (4), the effective value of $\bar{U}_T$ between 10 and 300 GeV could easily decrease by a factor of 2–3.

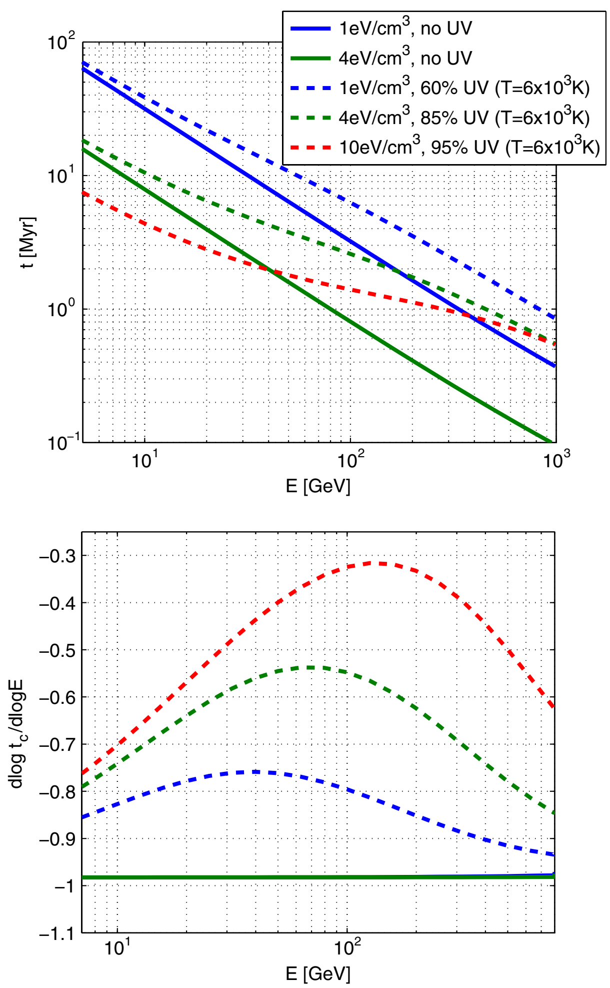

FIG. 4 (color online). Top: Cooling time t_c for $e^\pm$ radiative losses, as a function of $e^\pm$ energy, for different assumptions regarding the total electromagnetic energy density and its UV component. Bottom: Spectral index of the cooling time; the color scheme is the same as in the top.

We ignore bremsstrahlung (brem) and adiabatic losses. The brem optical depth can be estimated as $\tau_{\rm brem} \sim X_{\rm esc}/\zeta \approx 0.1(E/20\ {\rm GeV})^{-0.4}$, where $\zeta \sim 60$ g/cm^2 is the electron radiation length, and is too small to explain the e^+ loss inferred from Fig. 2. Adiabatic loss applies equally to e^+ and $\bar{p}$ and is thus constrained to be small by the $\bar{p}$ flux.

(2) The mean ISM density of the CR halo: We can now estimate the mean ISM density traversed by CRs. Using Eq. (2) together with Eqs. (3) and (4), we find

$$\bar{n}_{\rm ISM}(E/Z = 300\ {\rm GeV}) \gtrsim 1\left(\frac{\bar{U}_T}{1\ {\rm eV\,cm^{-3}}}\right){\rm cm}^{-3}, \quad (5)$$

$$\bar{n}_{\rm ISM}(E/Z = 10\ {\rm GeV}) \lesssim 0.15\left(\frac{\bar{U}_T}{1\ {\rm eV\,cm^{-3}}}\right){\rm cm}^{-3}, \quad (6)$$

assuming ISM composition of 90%H + 10%He by number.

Equations (5) and (6) suggest that the confinement volume of CRs decreases with increasing CR rigidity, to the extent that CRs at $E/Z \sim 300$ GeV spend much of their propagation time within the thin Galactic HI disc, with a scale height $h \simeq 200$ pc, while CRs at $E/Z \sim 10$ GeV probe a larger halo. These are not robust conclusions, however. For example, if a significant fraction of the grammage $X_{\rm esc}$ is accumulated during a short time in dense regions, e.g., near the CR source [32], then the halo could be larger. Energy dependence in $\bar{U}_T$ could further affect the interpretation. For example, $\bar{U}_T \propto E^{-0.6}$ (inspired by the CR grammage $X_{\rm esc} \propto E^{-0.4}$) would allow for a rigidity-independent $\bar{n}_{\rm ISM}$.

Finally, we comment that a rising f_{e^+} is comfortably compatible with the observed primary proton spectrum $J_p \propto E^{-2.8}$. It is clear from Fig. 4 that $t_{\rm esc}$ falling as $E^{-0.8}$ or so could lead to $t_c/t_{\rm esc}$, and thus to f_{e^+} that rise with increasing energy. Consider first the possibility that the CR halo decreases with increasing energy. As an example along this line [8], one-dimensional diffusion, with null boundary conditions at a CR scale height $L \propto E^{-0.4}$ and a rigidity-independent diffusion coefficient, would give $t_{\rm esc} \propto E^{-0.8}$, flat or rising f_{e^+}, and $X_{\rm esc} \propto E^{-0.4}$, consistent with observations. In this case, the inferred proton injection spectrum would be $\propto E^{-2.4}$. If, on the other hand, CR confinement occurs at a fixed volume, then the proton index could be interpreted as $E^{-0.8}$ softening by escape, on top of an E^{-2} injection. In this case, the slope of $X_{\rm esc} \propto E^{-0.4}$ would imply that the CR distribution is not homogeneous in the spallation region, with possible ramifications for gamma ray observations.

Conclusions.—The positron fraction measured by AMS-02 is consistent with the upper bound predicted in Ref. [8], assuming a secondary source. Upcoming AMS-02 measurements of the e^+ and $\bar{p}$ flux at yet higher energies will continue to test the model.

At the highest measurement energy, the positron flux saturates the upper bound, and throughout the measurement range, it is never smaller than a factor of $f_{e^+} \sim 0.3$ compared to it. We find this to be a compelling hint for a secondary source. Considering hypothetical primary sources such as pulsars or dark matter, we know of no intrinsic scale in these models that would fix the positron flux at this particular range.

Interpreted under the secondary source hypothesis, the positron data place interesting constraints on the propagation time of CRs at $E/Z \sim 10$–300 GeV that we roughly summarize by $t_{\rm esc}(10\ {\rm GeV}) \gtrsim 30$ Myr and $t_{\rm esc}(300\ {\rm GeV}) \lesssim 1$ Myr. The constraint on $t_{\rm esc}$ at $E/Z > 100$ GeV is obtained by the new positron data, with no direct counterpart in earlier CR data. The constraint at $E/Z \sim 10$ GeV is consistent, within uncertainties, with measurements of the elemental ratios of radioisotopes [8,17,18].

Using the measured CR grammage together with the new constraints on $t_{\rm esc}$, we derive the mean ISM particle density in the propagation region of high energy CRs $\bar{n}_{\rm ISM} \gtrsim 1\ {\rm cm}^{-3}$ for $E/Z = 300$ GeV. This result for $\bar{n}_{\rm ISM}$ is comparable to the mean ISM density in the Milky Way HI disc. At $E/Z = 10$ GeV, we find a smaller mean density $\bar{n}_{\rm ISM} \lesssim 0.15\ {\rm cm}^{-3}$. Put together, these numbers could mean that the scale height of the CR halo decreases with increasing CR rigidity [however, see the discussion following Eqs. (5) and (6) for alternative interpretations].

We thank Moti Milgrom, Kohta Murase, and Rashid Sunyaev for discussions. K. B. is supported by DOE Grant No. DE-FG02-90ER40542. B. K. is supported by the Bahcall Fellowship and by NASA through the Einstein Postdoctoral Fellowship awarded by the Chandra X-ray Center, which is operated by the Smithsonian Astrophysical Observatory for NASA under Contract No. NAS8-03060. E. W. is partially supported by GIF and UPBC grants.

*kblum@ias.edu
†boazka@ias.edu
‡eli.waxman@weizmann.ac.il

[1] M. Aguilar, G. Alberti, B. Alpat, A. Alvino, G. Ambrosi, K. Andeen, H. Anderhub, L. Arruda, P. Azzarello, A. Bachlechner *et al.* (AMS Collaboration), Phys. Rev. Lett. **110**, 141102 (2013).
[2] O. Adriani *et al.* (PAMELA Collaboration), Nature (London) **458**, 607 (2009).
[3] O. Adriani, G. C. Barbarino, G. A. Bazilevskaya, R. Bellotti, M. Boezio, E. A. Bogomolov, L. Bonechi, M. Bongi, V. Bonvicini, and S. Borisov, Astropart. Phys. **34**, 1 (2010).
[4] M. Ackermann *et al.* (Fermi LAT Collaboration), Phys. Rev. Lett. **108**, 011103 (2012).
[5] R. J. Protheroe, Astrophys. J. **254**, 391 (1982).
[6] I. Moskalenko and A. Strong, Astrophys. J. **493**, 694 (1998).
[7] T. Delahaye, J. Lavalle, R. Lineros, F. Donato, and N. Fornengo, Astron. Astrophys. **524**, A51 (2010).
[8] B. Katz, K. Blum, J. Morag, and E. Waxman, Mon. Not. R. Astron. Soc. **405**, 1458 (2010).
[9] J. J. Engelmann, P. Ferrando, A. Soutoul, P. Goret, and E. Juliusson, Astron. Astrophys. **233**, 96 (1990).
[10] W. R. Binns, T. L. Garrard, M. H. Israel, M. D. Jones, M. P. Kamionkowski, J. Klarmann, E. C. Stone, and C. J. Waddington, Astrophys. J. **324**, 1106 (1988).
[11] F. C. Jones, A. Lukasiak, V. Ptuskin, and W. Webber, Astrophys. J. **547**, 264 (2001).
[12] W. R. Webber, F. B. McDonald, and A. Lukasiak, Astrophys. J. **599**, 582 (2003).
[13] AMS-02 Collaboration, Proceedings of the ICRC2013, Rio de Janeiro, Brazil, 2013, http://www.cbpf.br/~icrc2013/; See also www.ams02.org.
[14] See Supplemental Material at http://link.aps.org/supplemental/10.1103/PhysRevLett.111.211101 for a derivation of CR grammage using recent AMS-02 B/C measurement to TV rigidity.
[15] O. Adriani, G. Bazilevskaya, G. Barbarino, R. Bellotti, M. Boezio *et al.*, JETP Lett. **96**, 621 (2013).
[16] A. Kounine, Int. J. Mod. Phys. E **21**, 1230005 (2012).
[17] W. R. Webber and A. Soutoul, Astrophys. J. **506**, 335 (1998).
[18] K. Blum, J. Cosmol. Astropart. Phys. 11 (2011) 037.
[19] N. E. Yanasak, M. E. Wiedenbeck, R. A. Mewaldt, A. J. Davis, A. C. Cummings, J. S. George, R. A. Leske, E. C. Stone, E. R. Christian, T. T. von Rosenvinge *et al.*, Astrophys. J. **563**, 768 (2001).
[20] H. S. Ahn, P. S. Allison, M. G. Bagliesi, J. J. Beatty, G. Bigongiari, P. J. Boyle, T. J. Brandt, J. T. Childers, N. B. Conklin, S. Coutu *et al.*, Astropart. Phys. **30**, 133 (2008).
[21] V. I. Zatsepin, A. D. Panov, N. V. Sokolskaya, J. H. Adams, H. S. Ahn, G. L. Bashindzhagyan, J. Chang, M. Christl, A. R. Fazely, T. G. Guzik *et al.*, Astron. Lett. **35**, 338 (2009).
[22] A. Obermeier, M. Ave, P. Boyle, Ch. Höppner, J. Hörandel, and D. Müller, Astrophys. J. **742**, 14 (2011).
[23] J. Lavalle, Mon. Not. R. Astron. Soc. **414**, 985 (2011).
[24] O. Adriani, G. C. Barbarino, G. A. Bazilevskaya, R. Bellotti, M. Boezio, E. A. Bogomolov, L. Bonechi, M. Bongi, V. Bonvicini, S. Borisov *et al.*, Science **332**, 69 (2011).
[25] A. Panov, J. Adams, H. Ahn, G. Bashinzhagyan, J. Watts *et al.*, Bull. Russ. Acad. Sci. Phys. **73**, 564 (2009).
[26] H. Ahn, P. Allison, M. Bagliesi, J. Beatty, G. Bigongiari *et al.*, Astrophys. J. **714**, L89 (2010).
[27] V. Ginzburg and V. Ptuskin, Rev. Mod. Phys. **48**, 161 (1976).
[28] V. S. Berezinskii, S. V. Bulanov, V. A. Dogiel, and V. S. Ptuskin, in *Astrophysics of Cosmic Rays*, edited by V. L. Ginzburg (North-Holland, Amsterdam, 1990).
[29] T. A. Porter and A. Strong, arXiv:astro-ph/0507119.
[30] R. Schlickeiser and J. Ruppel, New J. Phys. **12**, 033044 (2010).
[31] P. Blies and R. Schlickeiser, Astrophys. J. **751**, 71 (2012).
[32] R. Cowsik and B. Burch, Phys. Rev. D **82**, 023009 (2010).
[33] M. Ackermann *et al.* (Fermi LAT Collaboration), Phys. Rev. D **82**, 092004 (2010).